Numerical Assessment of Carbon Sequestration in a 3D Rhyolite Hosted Reservoir

Dale Emet Altar[1], Eylem Kaya[1] and Sadiq J. Zarrouk[1]

[1]Department of Engineering Science, University of Auckland, Private Bag 92019, Auckland, New Zealand

dalt507@aucklanduni.ac.nz

Keywords: *Carbon sequestration, Fluid-rock interaction, Reactive transport simulation, NCG, Rhyolite, TOUGHREACT™*

ABSTRACT

Carbon dioxide produced from geothermal operations may be captured and reinjected for safe and long-term storage to reduce emissions. However, this comes with key process challenges and potential reservoir management risks, requiring careful assessments during the technology testing phase and when gauging long-term resource performance.

The reaction of injected carbon dioxide with minerals in the reservoir formation to form carbonate minerals has the greatest capacity for storage permanence. A critical determinant for carbon mineralisation success is the reservoir rock; for example, the mineralisation of CO_2 in basaltic rocks rich in divalent cations, e.g. Ca^{2+} and Mg^{2+}, has been proven in Iceland. This work investigates the carbon sequestration potential in hydrothermal systems hosted in silicic rocks with lower divalent cation content, e.g., geothermal systems in New Zealand.

Numerical models were used in this study to assess carbon storage via mineralisation in a 3-dimensional hypothetical liquid-dominated geothermal reservoir hosted in rhyolite tuff, the corresponding sequestration potential, and the possible risks, e.g., breakthrough and surface leakage. Model results show that though mineralisation is expected during 40 years of concurrent mass extraction and CO_2 reinjection, <1% of the injected CO_2 was converted to carbonates during that period. After operations were discontinued, carbon dioxide mineralisation increased further to >12% in the subsequent 60 years of modelled time. Models to assess the effectivity of methods aimed at promoting mineralisation, i.e., adding divalent cations to the reinjected fluids or pH neutralisation, suggest short-term improvements in mineralisation rates but no significant effect in the long term.

1. INTRODUCTION

As of November 2023, atmospheric CO_2 levels have reached 420 ppm, with global temperatures at 0.89°C above pre-industrial averages, a trend driven by anthropogenic activities (NASA Jet Propulsion Laboratory, 2023). Projections indicate that without significant emission reductions, the median global temperature could rise to 3.28°C above pre-industrial levels by 2100 (Song et al., 2023). Climate change presents severe risks, including more frequent extreme weather events, droughts, and ice cover loss (IPCC, 2021), highlighting the urgent need for global efforts to reduce greenhouse gas emissions.

The energy production sector contributes significantly to greenhouse gas emissions, accounting for 78% globally (Stats NZ, 2018). While geothermal plants produce greenhouse gases (GHGs) such as CO_2 and trace amounts of CH_4 at a much lower rate compared to coal and natural gas (Fridriksson et al., 2016), emissions remain higher than from hydroelectric, wind, and nuclear power such that there remains an opportunity to reduce greenhouse gas emissions from geothermal operations.

Geologic sequestration has gained attention as an effective method for carbon storage. Supercritical CO_2 can be injected into saline aquifers and depleted oil and gas reservoirs, as reported by Kaszuba et al. (2003) and Knauss et al. (2005). In geothermal operations, CO_2 can be dissolved in brines and steam condensates for reinjection as a way to reduce greenhouse gas emissions. A notable success is the CarbFix project in Iceland, where CO_2-rich fluids are injected into basalt formations, leading to the formation of stable carbonate minerals (Gíslason et al., 2018; Ratouis et al., 2022; Sigfússon et al., 2018). In New Zealand, gas reinjection tests have been ongoing at the Ngā Tamariki Power Station since 2021, along with similar trials at Ngawha Generation and Te Huka Power Station (McLean et al., 2023).

CO_2 storage in reservoirs can occur through four mechanisms: direct physical trapping in its supercritical or gaseous phase ("structural trapping"), dissolved in the reservoir fluids ("dissolution trapping"), conversion to carbonate minerals upon reaction with the formation minerals and reservoir fluids ("mineralisation trapping") (Audigane et al., 2005), and residual or adsorption trapping (Kaya and Zarrouk, 2017). Mineralisation is considered the most effective for long-term storage (Matter and Kelemen, 2009; Ratouis et al., 2022), as indicated in Figure 1.

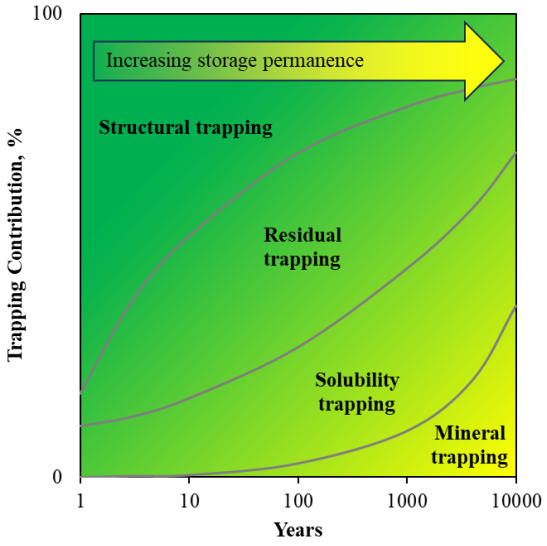


Figure 1: Estimated CO_2 trapping contribution of the various mechanisms as a function of time according to the IPCC (2005).

Reinjection of GHGs into geothermal reservoirs can reduce emissions and may also have a positive impact on maintaining reservoir pressure and enhancing steam production (Kaya and

Zarrouk, 2017). Dissolving CO_2 into reinjected fluids can lower pH, which may reduce mineral scaling rates and improve permeability through increased mineral dissolution in the formation (Gunnarsson and Arnórsson, 2005).

Assessing the technological challenges and reservoir management risks of CO_2 storage in geothermal reservoirs, such as breakthrough and surface leakage, is critical (Erol et al., 2022; Kaya et al., 2018). This study's comprehensive reservoir modelling approach consisted of two phases. The first phase focused on modelling the transport of geothermal water and CO_2 to predict CO_2 behaviour during production and reinjection. Key parameters were considered, including reservoir permeability, production and reinjection rates, and carbon dioxide injection rates. The second phase utilised a reactive transport model to assess the potential for permanent carbon storage through carbonate mineral formation. In both phases, the production of geothermal fluids was modelled along with brine and steam condensate reinjection for 40 years of field operations in a typical single flash steam power plant.

The first phase results indicate that >99% of injected carbon dioxide for sequestration is trapped through dissolution during the modelled 40 years of field operations. Returns of reinjected brine with dissolved NCG resulted in higher CO_2 content in the produced geothermal fluids over time. Structural trapping was not observed in the modelled scenarios as CO_2 did not exist as a separate phase in the modelled reservoir. Altar et al. (2024) report these in more detail, and the reader is referred to their work.

This paper will focus primarily on the implications of mineralisation on carbon storage. Model scenarios explored various parameters impacting sequestration behaviour and reservoir performance.

2. REACTIVE TRANSPORT MODEL

The models for the hypothetical reservoir were set up using the numerical simulation tool TOUGHREACT™ version 4 (Sonnenthal et al., 2021). The fluid equation of state EOS2 was used for the flow and reactive transport models which provides fluid properties for water and carbon dioxide solutions for applications in gas-rich reservoirs.

2.1 Transport Parameters

The 3D rectangular grid structure covers a total area of 34 km × 28 km with a depth of 6 km. The grid structure is shown in Figure 2. The smallest grid blocks, used within the reservoir area of interest, have dimensions of 500 m × 500 m to achieve better resolution in the region covering production and injection zones balanced against the computational load for the models.

All model blocks are single porosity. Eight rock types were used in the model to capture the permeability heterogeneity in a volcanic-hosted geothermal system and represent key features. Boundary blocks of the modelled reservoir were assigned volumes $\geq 10^{50}$ m^3 to define constant pressure, temperature and chemistry boundaries. The full details of the grid structure are discussed in Altar et al. (2024).

The model was run without fluid-rock interactions to reach a stable natural state before running analytical scenarios. Upflow rates for both water and CO_2 were specified for natural state modelling and assigned to four adjacent blocks, also indicated in Figure 2. The reservoir fluid was assumed to have a CO_2 content of 0.014 mol/kg, with combined mass flow rates of 100 kg/s for water and 0.0616 kg/s for CO_2.

For the production scenarios, geothermal fluids were produced from four grid blocks positioned at a depth of 1200 m. Brine and condensate from the production process were reinjected at grid blocks located at 1600 m depth, approximately 2 km horizontal distance away from the production blocks. Their locations are indicated in Figure 3. Production from each block was modelled using DELV generators using a productivity index (PI) of 4.7×10^{-12} m^3 so that production over time is a function of well deliverability and reservoir pressure. Wellbore pressures at the production feed zone depth were estimated using wellbore simulations.

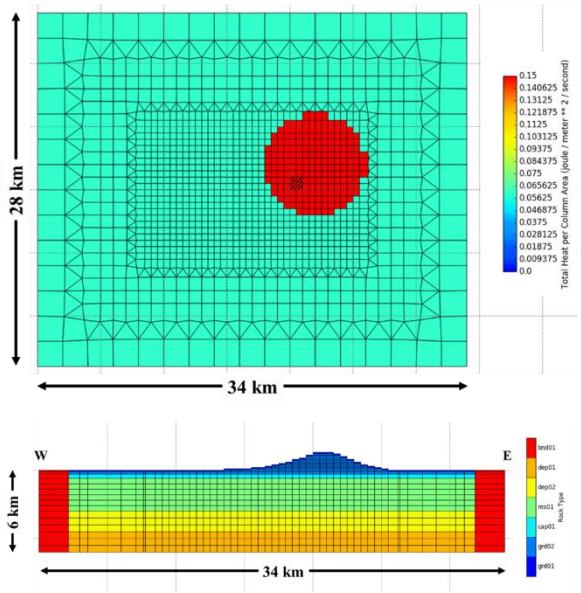


Figure 2: The model grid structure showing the bottom layer with colours representing the heat fluxes (W/m^2) assigned and a W-E Slice view of the model grid structure indicating the rock types. The hatched red area in the bottom view indicates the position of the mass upflow, covering four adjacent grid blocks.

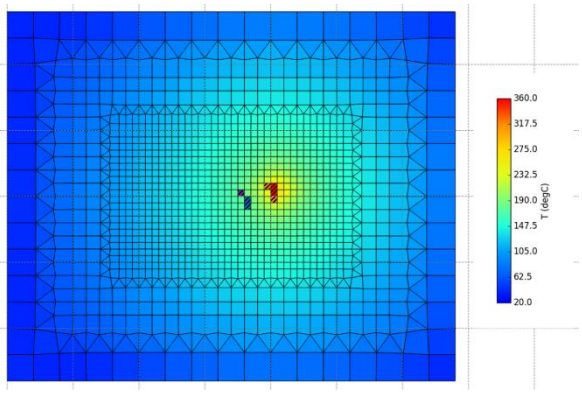


Figure 3: Model layer at 1200 m depth. Colours represent the block temperatures. Hatched red and orange areas indicate where fluids are produced. The hatched violet area indicates the condensate injection block location, while the hatched blue regions correspond to the brine injection blocks, all at a depth of 1600 m.

Brine and condensate reinjection rates were estimated from mass production rates assuming a single flash (5.5 bar) process, as shown in Figure 4. The flashed steam is utilised for electrical power generation while the separated brine is reinjected. A fraction of the condensed steam is likewise reinjected, approximately 20%, according to Kamila et al. (2021) and Rivera Diaz et al. (2016).

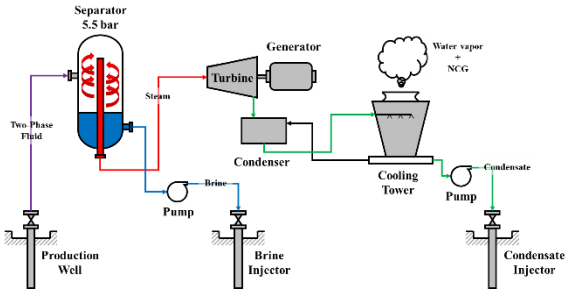


Figure 4: Process flow diagram for the hypothetical single flash geothermal plant.

2.2 Geochemical Parameters

The reservoir was assumed to be hosted in an altered rhyolite ignimbrite formation for reactive transport. The modelled petrography was adapted from literature, primarily from Youngman (1988). Components of the formations that were not identified as specific mineral phenocrysts were represented as glass, including groundmass. Hydrothermal minerals were assumed to have replaced 50% of the original materials. Additional data for the alteration minerals were adapted from Bignall (1991), Cattell (2015), Chernet (1987), Rosenberg (2017) and Struthers (2019). Whole sample oxide analyses were used to represent the glass composition. The modelled mineralogy and corresponding abundances are given in Table 1. Additional carbonate, clay and silica minerals that are expected to form under reinjection conditions were included. Siderite, dolomite and ankerite were considered along with calcite and magnesite for carbon mineralisation based on the work of other investigators (Van Pham et al., 2012; Van Pham et al., 2011; Xu et al., 2005). Reactive calculations were limited to the main reservoir lithology, represented by rock type "res01". This was implemented to optimise computational resources and time.

Mineral reactions were primarily modelled to follow kinetic constraints, except for calcite, magnesite, siderite, dolomite, ankerite and rutile, which were assumed to be under local equilibrium. Parameters used to calculate the dissolution rate constants (the reaction rate constant at 25°C, k_{25}, and the activation energy, Ea) were primarily adapted from Palandri and Kharaka (2004). Kinetic parameters for microcline and hypersthene were adapted from those for K-feldspar and augite, respectively. Dissolution kinetics following the work of Köhler et al. (2003) was implemented for illite and Kiryukhin et al. (2004) for wairakite. The dissolution rate parameters at neutral pH represented precipitation kinetics for secondary minerals.

The reactive surface area (RSA) for fractured media was estimated using the methods described by Xu et al. (2014). The parameters needed for the calculation were adapted from the works of McLean and McNamara (2011) and McNamara et al. (2019). Values for each mineral were reduced by three orders of magnitude for use with the model to account for the general observation that field reaction rates are orders slower than laboratory rates (Aradóttir et al., 2012; White and Brantley, 2003).

Table 1: Mineralogy and corresponding volume fractions for the modelled reservoir.

	MINERAL	% VOL
PRIMARY	Quartz	10.91%
	Anorthite	3.10%
	Albite	7.06%
	Microcline	0.18%
	Hypersthene	0.84%
	Glass	35.68%
SECONDARY	Illite	14.71%
	Calcite	3.09%
	Magnetite	1.93%
	K-Feldspar	2.08%
	Chlorite	8.28%
	Epidote	6.11%
	Pyrite	1.86%
	Rutile	2.08%
	Wairakite	2.08%
	Magnesite, Siderite, Dolomite, Ankerite, Ilmenite, Smectite-Ca-K, Am-Silica, Chalcedony and Kaolinite	0.00%

Reaction equilibrium data were adapted from the EQ3/6 database (Wolery et al., 2007). The porosity-permeability function was modelled following the Verma-Pruess relation as implemented in TOUGHREACT™. The critical porosity was set to 8.5% and the exponent n to a value of 2. This enables an assessment of the effects of fluid-rock interaction on permeability.

2.3 Modelling Scenarios

First, a model was run for 40 years without production or injection ("Undeveloped" scenario). The reservoir fluid is not initially in equilibrium with the reservoir minerals in all blocks due to temperature variations within the reservoir. Therefore, alteration processes occur as reservoir fluids circulate. This scenario also accounts for the effect of CO_2 already present in the upflow. All subsequent model runs were compared against the results of the Undeveloped scenario to ascertain whether the observed alterations were induced by production and injection rather than inherent reservoir processes.

A passive NCG reinjection scenario was also run ("Baseline" scenario), assuming the plant is operated as a typical flash plant where gases are separated from steam condensates and vented, and the reinjected brine and condensate have lower gas content. The active NCG reinjection scenario used for comparison involved saturating the brine and condensate with CO_2 at 40 bar pressure ("40-BC" scenario). Saturated CO_2 dissolution was modelled following Henry's Law, where the Henry's law coefficient for CO_2 is dependent on temperature and the ionic strength of the solution based on the formulation by Battistelli et al. (1997). Model scenarios involved an initial 40 years of concurrent production and reinjection, after which production ceased, and the models were run for an additional 60 years to track how the injected carbon dioxide behaved over time.

3. RESULTS AND DISCUSSION

The region of analytical interest for the reactive models is indicated in Figure 5.

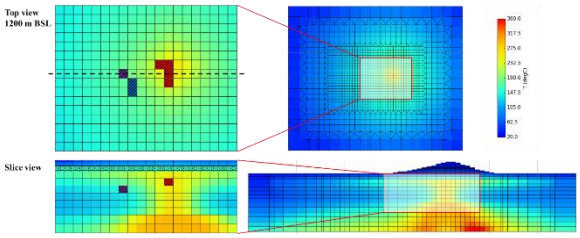


Figure 5: Top view at 1200 m BSL and slice view of the region of interest in the modelled reservoir, showing the initial block temperatures.

Results of the Undeveloped and Baseline scenarios within this region show that calcite, glass and quartz have observable changes in volume fractions resulting from the modelled chemical reactions in 40 years of field development. In the 40-BC scenario, both ankerite and siderite formed, while dolomite formed in all three scenarios. The results for calcite are shown in Figure 6.

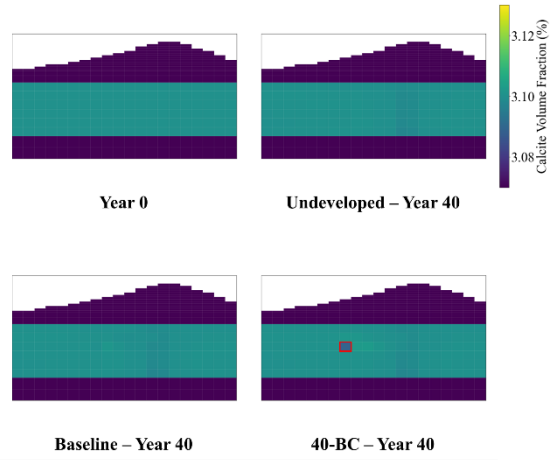


Figure 6: Modelled results for calcite abundance for the Undeveloped, Baseline and 40-BC scenarios after 40 years. The block boxed in red is the condensate injection block.

Calcite dissolved in the condensate and brine injection blocks in the 40-BC scenario, while calcite deposition was observed in the adjacent grid blocks. Due to the number of blocks and the variations in the effect of fluid-rock interactions on carbonate mineral abundance, the impact of CO_2 injection was assessed based on a large reservoir sector where critical flow processes and chemical interactions occur. To constrain the calculations, the grid blocks in the region indicated in Figure 5 were considered, further limited to the blocks within the reservoir (from 600 m to 3000 m depth). Calcite, magnesite, siderite, ankerite and dolomite were included in the analysis.

First, the net change in mineral volumes from the alteration processes was calculated relative to their original volumes. The calculated volumes were then converted to mineral moles using the minerals' respective molar volumes, which are then used to calculate the moles of equivalent CO_2. For calcite, magnesite and siderite, one mole of the mineral is equivalent to one mole of CO_2. In comparison, one mole of either ankerite or dolomite is equivalent to two moles of CO_2 based on chemical stoichiometry. Finally, the mass of equivalent carbon dioxide sequestered (m_{CO2}, tonne) through mineralisation was calculated.

The results of the calculations for each scenario after 40 years are summarised in Table 2. The 40-BC scenario produced the highest mass of equivalent CO_2 sequestered by mineralisation. Notably, calcite and dolomite form in the modelled reservoir for the Undeveloped scenario due to alteration processes between the circulating fluids, the carbon dioxide naturally present in the reservoir fluids and the reservoir minerals. Subtracting the equivalent CO_2 mass from mineralisation in the Undeveloped scenario from both the Baseline and 40-BC scenarios results in values that are descriptive of the incremental effect of field operations on mineralisation.

Table 2: Equivalent carbon dioxide masses, in metric tonnes, from carbonate mineral deposition for the Undeveloped, Baseline and 40-BC model scenarios.

CO_2, TONNES	UNDEVELOPED	BASELINE	40-BC
CALCITE	1.16E+05	1.15E+05	1.04E+05
MAGNESITE	-	-	-
SIDERITE	-	-	3.26E+03
ANKERITE	-	-	2.41E+04
DOLOMITE	1.68E+04	1.59E+04	1.97E+04
TOTAL	1.33E+05	1.31E+05	1.51E+05

The resulting values are -1,959 tonnes and 18,080 tonnes for the Baseline and 40-BC scenarios, respectively, implying that passive NCG reinjection results in a net mobilisation of carbon dioxide in the reservoir, while active NCG injection results in sequestration. Given that the net mass of CO_2 injected into the reservoir for the model is 2.52×10^6 tonnes (Altar et al., 2024), only 0.72% of injected CO_2 was converted to carbonate minerals in scenario 40-BC. This suggests that dissolution (>99% of CO_2) is the primary sequestration mechanism during the 40 years of operation.

Of the three scenarios, siderite and ankerite only formed under scenario 40-BC. This is associated with increased glass alteration for this scenario (Figure 7). The additional glass dissolution in scenario 40-BC is promoted by acidic injectates due to higher carbon dioxide concentrations, resulting in iron mobilisation (along with aluminium, silica, potassium and magnesium).

Lower fluid pH due to dissolved carbon dioxide promotes primary mineral dissolution, increasing the aqueous concentrations of the divalent cations Ca^{2+}, Mg^{2+} and Fe^{2+} (Gysi and Stefánsson, 2011), which subsequently form carbonate minerals with CO_2. Basalt is generally considered a good candidate for carbonate mineralisation because of its high divalent cation content (Clark et al., 2020). In the tholeiite basalt studied by Altar et al. (2022) and Altar et al. (2023), the Ca, Mg and Fe moles per mole of SiO_2 are 0.24, 0.20 and 0.23 (0.67 total); basalts in the Taupo Volcanic Zone range in total divalent cation content from 0.5 to 0.7 (Gamble et al., 1990). In contrast, the corresponding Ca, Mg and Fe moles per mole of SiO_2 in the rhyolitic ignimbrite considered in this study are only 0.03, 0.01 and 0.01 (0.05 total) (Youngman, 1988).

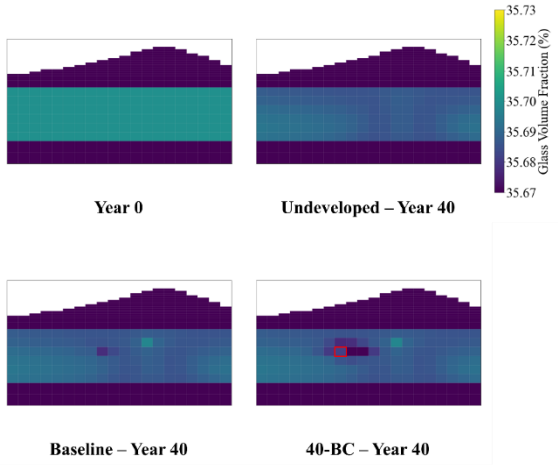


Figure 7: Modelled results for glass abundance for the Undeveloped, Baseline and 40-BC scenarios after 40 years. The block boxed in red is the condensate injection block.

If CO_2 remains in solution due to limited mineralisation, there is a risk of returns to production. The modelled CO_2 concentrations for Phase 1 and 2 of scenario 40-BC after 40 years are shown in Figure 8. Using the non-reactive model in Phase 1, the trend of CO_2 concentration over time in the modelled grid blocks indicates returns to the production area (Altar et al., 2024). Some of the injected carbon dioxide also migrate away from the production area. The reactive transport model indicates a similar trend. Whereas the CO_2 content in the steam is expected to decrease over time for the Baseline scenario based on the Phase 1 study, the 40-BC scenario will result in higher NCG content in the flashed steam over time, necessitating a future assessment of the impact on turbine efficiency. Surface leakage is not expected during the 40-year production period for the reservoir properties defined.

Kaya and Lynne (2023) suggest that carbon mineralisation in non-ideal formations may be improved by introducing additional cations into the reinjected fluids or by neutralising the fluids to increase the amount of dissolved carbon dioxide. Initial explorations of these options were carried out through two further iterations of the 40-BC scenario. Considering the materials and energy needed to alter the injectate chemistry, only the condensate was modified in the additional reactive model scenarios. In the "40-BC-Cations" scenario, the Ca^{2+}, Mg^{2+}, and Fe^{2+} cation concentrations in the CO_2-saturated condensate were individually increased to 0.001 mol/kg from <0.00025 mol/kg. The scenario "40-BC-Neutralised" involved neutralising the CO_2-saturated condensate to a pH of 7.

The values for net carbon dioxide stored as minerals relative to the Undeveloped scenario increased to 42,220 tonnes for scenario 40-BC-Cations and 28,190 tonnes for scenario 40-BC-Neutralised, corresponding to 1.68% and 1.12% of the injected carbon dioxide after 40 years of field operations. Mineralisation improved compared to simply injecting condensates saturated with CO_2.

Figure 9 shows the total carbonate mineral volume fractions after 40 years for both scenarios compared to 40-BC. The 40-BC-Cation results show similar dissolution-precipitation patterns to 40-BC but with higher volumes of deposited carbonate minerals. The net increase in mineralised carbon in the 40-BC-Neutralised scenario is due to secondary carbonate deposition and reduced calcite dissolution in the injection blocks. Overall, the results of the additional scenarios suggest the feasibility of improving overall mineralisation rates in otherwise non-ideal reservoir lithologies by introducing additional divalent cations to the injected water or through neutralisation. However, additional analytical work is needed to ascertain these findings and assess options to combine both treatments optimally, considering economic feasibility.

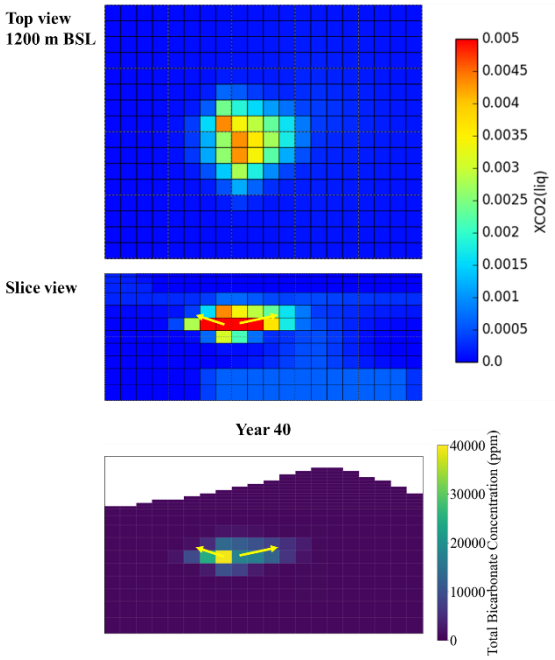


Figure 8: Modelled block CO_2 concentrations from Phase 1 of the study, shown in the upper figures (Altar et al., 2024) and the results from the reactive transport models of Phase 2 in the bottom figure. Arrows indicate the transport path of injected CO_2.

The modelled mineralisation results during 40 years of field operations generally agree with the estimated time scales versus trapping contribution for mineralisation trapping shown in Figure 1 (IPCC, 2005). According to the figure, time scales may range from hundreds to thousands of years, and even then, less than 50% of the initially injected CO_2 mass may be stored as carbonate minerals. However, Clark et al. (2020) reported that up to 95% of the injected carbon in the original CarbFix site was mineralised in less than two years (basalt rocks at 20°C to 50°C conditions), while in the CarbFix2 site, more than 50% was mineralised within four months in a basalt reservoir at temperatures higher than 250°C. Given favourable chemical conditions, sufficient mineralisation may occur in time scales of months to years rather than hundreds to thousands of years.

To gauge further mineralisation beyond 40 years of field development in the hypothetical reservoir, the reactive transport models for scenarios 40-BC, 40-BC-Cations, and 40-BC-Neutralised were extended by 60 years without further extraction or reinjection. In that time, carbonate minerals continued to form (Figure 9), resulting from continuing interactions of the reservoir minerals with the CO_2-rich injectates. Mineralisation rates were calculated; 12.86% of

the injected CO_2 was mineralised in the 40-BC case, 13.49% for the 40-BC-Cations case, and 12.15% in the 40-BC-Neutralised case. The slight differences in long-term mineralisation rates between scenarios suggest that the improvements from dissolving additional cations into the injectates or pH modification are more critical for accelerating short-term mineralisation but may have a limited impact on long-term sequestration.

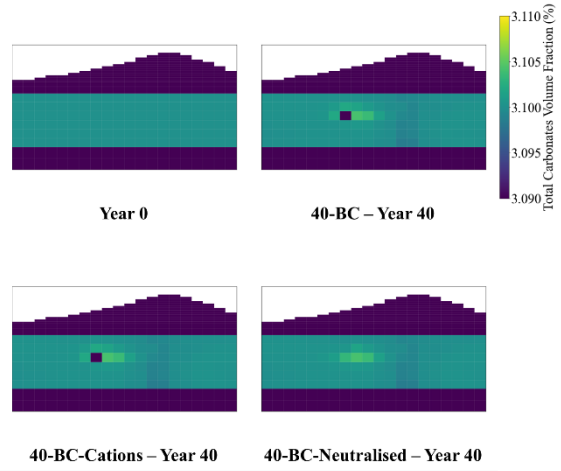


Figure 9: Modelled total carbonate mineral abundance results for the 40-BC, 40-BC-Cation and 40-BC-Neutralised scenarios after 40 years.

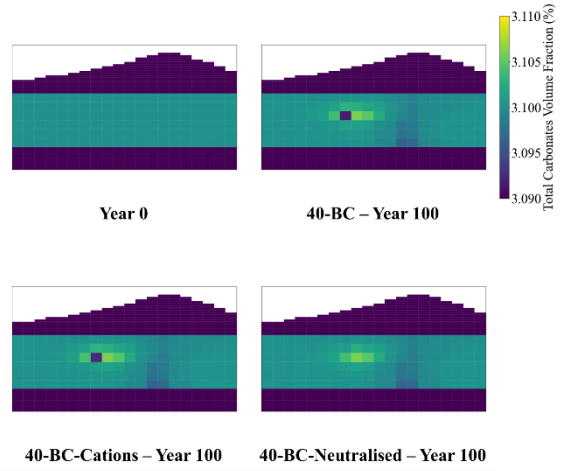


Figure 10: Modelled total carbonate mineral abundance results for the 40-BC, 40-BC-Cation and 40-BC-Neutralised scenarios after 100 years.

Residual, or adsorption, sequestration was not modelled. Despite this, it is worth mentioning that carbon dioxide has been observed to adsorb onto mica (Bhattacharyya, 1989), montmorillonite (Giesting et al., 2012), kaolinite (Chen and Lu, 2015) and illite (Heller and Zoback, 2014). However, experimental data on CO_2 adsorption are limited and are commonly measured at temperatures below 100°C. This limits the ability to include adsorption parameters in the reactive transport models for geothermal applications.

As a last point of discussion, though the reactive models accounted for effects on porosity and permeability, the porosity changes modelled did not result in significant permeability changes.

4. CONCLUSIONS

The study results showed that carbon storage in a geothermal reservoir hosted in rhyolite ignimbrite through mineralisation trapping is feasible. Mineralisation was observed in 40 years of field operations with concurrent CO_2 injection through the brine and condensate; however, the amount trapped is less than 1% of the injected mass due to the low cation content in the rhyolitic reservoir rock. More than 99% of injected carbon dioxide for sequestration was trapped through dissolution. The mineralisation rate improved after adding divalent cations, i.e. Ca^{2+}, Mg^{2+} and Fe^{2+}, to the reinjected fluids or by pH neutralisation.

Depending on the connectivity of the reinjection and production sectors, injected carbon dioxide may communicate and be produced with steam or two-phase fluids if insufficient mineralisation occurs. This risk decreases the efficiency of the sequestration process and should be considered in future work. It will likely also affect the power generation process as turbine efficiencies may degrade with higher NCG mass fractions in the flashed steam. Other potential impacts related to reservoir pressure, fluid enthalpy, and productivity should likewise be analysed, though they were not observed in the reservoir model for this study.

Further mineralisation was predicted by the models after mass extraction and reinjection had stopped. The amount of mineralised CO_2 increased to more than 12% of the total mass sequestered in the 40-BC scenario, including the scenarios with process improvements. The modelled results suggest that the benefits from dissolving additional cations into the injectates or pH modification are more critical when targeting rapid and short-term mineralisation but may have a limited impact on long-term sequestration.

The importance of developing appropriate baseline scenarios when assessing outcomes for mineralisation was demonstrated. In this study, carbonates form even without the effects of field development, occurring directly from the interaction of reservoir fluids with the formation minerals. Overestimation of storage capacity and impacts may arise if baseline interaction scenarios are not considered in the scope of investigations.

Future studies should assess the effects of other NCGs, e.g., H_2S and O_2, which may be present with carbon dioxide and can affect the evolution of fluid chemistry and the mode of mineral alteration. Longer-term model runs and structural influences on reservoir flow path behaviour should also be incorporated into investigation scenarios to provide a more detailed and realistic assessment of carbon sequestration dynamics in geothermal reservoirs.

ACKNOWLEDGEMENTS

This work was supported by the University of Auckland Doctoral Scholarship. We also thank the NZ Ministry of Business, Innovation and Employment for funding the work through the MBIE Research Programme: UOAX2211 “Reversing Carbon Emissions in the Geothermal Energy Industry: Template for Emission-Intensive Industries” projects.

REFERENCES

Altar, D. E., Kaya, E., Zarrouk, S. J., Passarella, M. & Mountain, B. W., (2022). Numerical geochemical modelling of basalt-water interaction under subcritical conditions. *Geothermics*, *105*, 102520.

https://doi.org/https://doi.org/10.1016/j.geothermics.2022.102520

Altar, D. E., Kaya, E., Zarrouk, S. J., Passarella, M. & Mountain, B. W., (2023). Reactive transport modelling under supercritical conditions. *Geothermics*, *111*, 102725. https://doi.org/https://doi.org/10.1016/j.geothermics.2023.102725

Altar, D.E., Kaya, E., Zarrouk, S.J., (2024). Structural and Dissolution Trapping of Carbon in Geothermal Reservoirs: A Numerical Assessment. *In: Proceedings, 49th Workshop on Geothermal Reservoir Engineering*.

Aradóttir, E. S. P., Sonnenthal, E. L. & Jónsson, H., (2012). Development and evaluation of a thermodynamic dataset for phases of interest in CO_2 mineral sequestration in basaltic rocks. *Chemical Geology*, *304-305*, 26-38. https://doi.org/https://doi.org/10.1016/j.chemgeo.2012.01.031

Audigane, P., Gaus, I., Pruess, K. & Xu, T., (2005). Reactive transport modeling using TOUGHREACT for the long term CO_2 storage at Sleipner, North Sea. *In Proceedings: 4th Annual Conference on Carbon Capture and Sequestration DOE/NETL*.

Battistelli, A., Calore, C. & Pruess, K., (1997). The simulator TOUGH2/EWASG for modelling geothermal reservoirs with brines and non-condensible gas. *Geothermics*, *26*(4), 437-464.

Bhattacharyya, K. G., (1989). Adsorption of carbon dioxide on mica surfaces. *Langmuir*, *5*(5), 1155-1162. https://doi.org/https://doi.org/10.1021/la00089a005

Bignall, G., (1991). Subsurface Stratigraphy and Structure of the OrakeiKorako and Te Kopia Geothermal Systems, New Zealand. *In Proceedings: 13th New Zealand Geothermal Workshop*.

Cattell, H., (2015). *Volcanic evolution of the Huka Group at Wairakei-Tauhara Geothermal Field, Taupo Volcanic Zone, New Zealand* (Publication Number 2124076) [PhD, University of Canterbury]. Christchurch, New Zealand.

Chen, Y.-H. & Lu, D.-L., (2015). CO_2 capture by kaolinite and its adsorption mechanism. *Applied Clay Science*, *104*, 221-228. https://doi.org/https://doi.org/10.1016/j.clay.2014.11.036

Chernet, T., (1987). *Lithic inclusions in the Taupo Pumice Formation* [MSc, Te Herenga Waka-Victoria University of Wellington]. Wellington, New Zealand.

Clark, D. E., Oelkers, E. H., Gunnarsson, I., Sigfússon, B., Snæbjörnsdóttir, S. Ó., Aradóttir, E. S. & Gíslason, S. R., (2020). CarbFix2: CO_2 and H_2S mineralisation during 3.5 years of continuous injection into basaltic rocks at more than 250 °C. *Geochimica et Cosmochimica Acta*, *279*, 45-66. https://doi.org/https://doi.org/10.1016/j.gca.2020.03.039

Erol, S., Akın, T., Başer, A., Saraçoğlu, Ö. & Akın, S., (2022). Fluid-CO_2 injection impact in a geothermal reservoir: Evaluation with 3-D reactive transport modeling. *Geothermics*, *98*, 102271. https://doi.org/https://doi.org/10.1016/j.geothermics.2021.102271

Fridriksson, T., Mateos, A., Audinet, P. & Orucu, Y., (2016). *Greenhouse Gases from Geothermal Power Production*.

Gamble, J. A., Smith, I. E. M., Graham, I. J., Peter Kokelaar, B., Cole, J. W., Houghton, B. F. & Wilson, C. J. N., (1990). The petrology, phase relations and tectonic setting of basalts from the taupo volcanic zone, New Zealand and the Kermadec Island arc - Havre trough, SW Pacific. *Journal of Volcanology and Geothermal Research*, *43*(1), 253-270. https://doi.org/https://doi.org/10.1016/0377-0273(90)90055-K

Giesting, P., Guggenheim, S., Koster van Groos, A. F. & Busch, A., (2012). Interaction of carbon dioxide with Na-exchanged montmorillonite at pressures to 640bars: Implications for CO_2 sequestration. *International Journal of Greenhouse Gas Control*, *8*, 73-81. https://doi.org/https://doi.org/10.1016/j.ijggc.2012.01.011

Gíslason, S. R., Sigurdardóttir, H., Aradóttir, E. S. & Oelkers, E. H., (2018). A brief history of CarbFix: Challenges and victories of the project's pilot phase. *Energy Procedia*, *146*, 103-114. https://doi.org/https://doi.org/10.1016/j.egypro.2018.07.014

Gunnarsson, I. & Arnórsson, S., (2005). Treatment of geothermal waste water to prevent silica scaling. *In Proceedings: World Geothermal Congress 2005*.

Gysi, A. P. & Stefánsson, A., (2011). CO_2–water–basalt interaction. Numerical simulation of low temperature CO_2 sequestration into basalts. *Geochimica et Cosmochimica Acta*, *75*(17), 4728-4751. https://doi.org/https://doi.org/10.1016/j.gca.2011.05.037

Heller, R. & Zoback, M., (2014). Adsorption of methane and carbon dioxide on gas shale and pure mineral samples. *Journal of Unconventional Oil and Gas Resources*, *8*, 14-24. https://doi.org/https://doi.org/10.1016/j.juogr.2014.06.001

IPCC, (2005). *IPCC special report on carbon dioxide capture and storage*. Cambridge University Press.

IPCC, (2021). Summary for Policymakers. In Masson-Delmotte, V., Zhai, P., Pirani, A., Connors, S. L., Péan, C., Berger, S., Caud, N., Chen, Y., Goldfarb, L., Gomis, M. I., Huang, M., Leitzell, K., Lonnoy, E., Matthews, J. B. R., Maycock, T. K., Waterfield, T., Yelekçi, O., Yu, R., & Zhou, B. (Eds.), *Climate Change 2021: The Physical Science Basis. Contribution of Working Group I to the Sixth Assessment Report of the Intergovernmental Panel on*

Climate Change (pp. 3−32). Cambridge University Press. https://doi.org/10.1017/9781009157896.001

Kamila, Z., Kaya, E. & Zarrouk, S. J., (2021). Reinjection in geothermal fields: An updated worldwide review 2020. *Geothermics*, *89*, 101970. https://doi.org/https://doi.org/10.1016/j.geothermics.2020.101970

Kaszuba, J.P., Janecky, D.R., Snow, M.G., (2003). Carbon dioxide reaction processes in a model brine aquifer at 200 °C and 200 bars: implications for geologic sequestration of carbon. *Applied Geochemistry 18* (7), 1065–1080. https://doi.org/10.1016/S0883-2927(02)00239-1

Kaya, E., Callos, V. & Mannington, W., (2018). CO_2 –water mixture reinjection into two-phase liquid dominated geothermal reservoirs. *Renewable Energy*, *126*, 652-667. https://doi.org/https://doi.org/10.1016/j.renene.2018.03.067

Kaya, E. & Lynne, B. Y., (2023). Reversing carbon emissions in the geothermal energy industry project: A geoscience perspective. *In Proceedings: 45th New Zealand Geothermal Workshop*. Auckland, New Zealand.

Kaya, E. & Zarrouk, S. J., (2017). Reinjection of greenhouse gases into geothermal reservoirs. *International Journal of Greenhouse Gas Control*, *67*, 111-129. https://doi.org/https://doi.org/10.1016/j.ijggc.2017.10.015

Kiryukhin, A., Xu, T., Pruess, K., Apps, J. & Slovtsov, I., (2004). Thermal–hydrodynamic–chemical (THC) modeling based on geothermal field data. *Geothermics*, *33*(3), 349-381. https://doi.org/https://doi.org/10.1016/j.geothermics.2003.09.005

Knauss, K. G., Johnson, J. W. & Steefel, C. I., (2005). Evaluation of the impact of CO_2, co-contaminant gas, aqueous fluid and reservoir rock interactions on the geologic sequestration of CO_2. *Chemical Geology*, *217*(3), 339-350. https://doi.org/http://doi.org/10.1016/j.chemgeo.2004.12.017

Köhler, S. J., Dufaud, F. & Oelkers, E. H., (2003). An experimental study of illite dissolution kinetics as a function of ph from 1.4 to 12.4 and temperature from 5 to 50°C. *Geochimica et Cosmochimica Acta*, *67*(19), 3583-3594. https://doi.org/https://doi.org/10.1016/S0016-7037(03)00163-7

Matter, J. M. & Kelemen, P. B., (2009). Permanent storage of carbon dioxide in geological reservoirs by mineral carbonation. *Nature Geoscience*, *2*(12), 837-841. https://doi.org/https://doi.org/10.1038/ngeo683

McLean, K., Montague, T., Alcaraz, S., Daysh, S., Doorman, P., Luketina, K., Tsui, K., White, B. & Zarrouk, S. J., (2023). 2020-2023 New Zealand Country Update. *In Proceedings: World Geothermal Congress 2023*. Beijing, China.

McLean, K. & McNamara, D. D., (2011). Fractures interpreted from acoustic formation imaging technology: correlation to permeability. *In Proceedings: 36th Workshop on Geothermal Reservoir Engineering*.

McNamara, D. D., Milicich, S. D., Massiot, C., Villamor, P., McLean, K., Sépulveda, F. & Ries, W. F., (2019). Tectonic Controls on Taupo Volcanic Zone Geothermal Expression: Insights From Te Mihi, Wairakei Geothermal Field. *Tectonics*, *38*(8), 3011-3033.

NASA Jet Propulsion Laboratory. 2023. Carbon Dioxide. In (Vol. 2024).

Palandri, J. L. & Kharaka, Y. K., (2004). *A Compilation of Rate Parameters of Water-Mineral Interaction Kinetics for Application to Geochemical Modeling*.

Ratouis, T. M. P., Snæbjörnsdóttir, S. Ó., Voigt, M. J., Sigfússon, B., Gunnarsson, G., Aradóttir, E. S. & Hjörleifsdóttir, V., (2022). Carbfix 2: A transport model of long-term CO_2 and H_2S injection into basaltic rocks at Hellisheidi, SW-Iceland. *International Journal of Greenhouse Gas Control*, *114*, 103586. https://doi.org/https://doi.org/10.1016/j.ijggc.2022.103586

Rivera Diaz, A., Kaya, E. & Zarrouk, S. J., (2016). Reinjection in geothermal fields − A worldwide review update. *Renewable and Sustainable Energy Reviews*, *53*, 105-162. https://doi.org/https://doi.org/10.1016/j.rser.2015.07.151

Rosenberg, M., (2017). *Volcanic and tectonic perspectives on the age and evolution of the Wairakei-Tauhara geothermal system* [PhD, Te Herenga Waka-Victoria University of Wellington]. Wellington, New Zealand.

Sigfússon, B., Arnarson, M. Þ., Snæbjörnsdóttir, S. Ó., Karlsdóttir, M. R., Aradóttir, E. S. & Gunnarsson, I., (2018). Reducing emissions of carbon dioxide and hydrogen sulphide at Hellisheidi power plant in 2014-2017 and the role of CarbFix in achieving the 2040 Iceland climate goals. *Energy Procedia*, *146*, 135-145. https://doi.org/https://doi.org/10.1016/j.egypro.2018.07.018

Song, J., Tong, G., Chao, J., Chung, J., Zhang, M., Lin, W., Zhang, T., Bentler, P. M. & Zhu, W., (2023). Data driven pathway analysis and forecast of global warming and sea level rise. *Scientific Reports*, *13*(1), 5536. https://doi.org/https://doi.org/10.1038/s41598-023-30789-4

Sonnenthal, E., Spycher, N., Xu, T. & Zheng, L., (2021). *TOUGHREACT V4. 12-OMP and TReactMech V1. 0 Geochemical and Reactive-Transport User Guide*.

Stats NZ, (2018). *Global greenhouse gas emissions*.

Struthers, J., (2019). *Comparison of geothermal structures at Tauhara Geothermal Field, New Zealand and Muara Laboh, Indonesia*.

Van Pham, T. H., Aagaard, P. & Hellevang, H., (2012). On the potential for CO_2 mineral storage in continental flood basalts–PHREEQC batch- and 1D diffusion–reaction simulations. *Geochemical Transactions*, *13*(1), 5. https://doi.org/https://doi.org/10.1186/1467-4866-13-5

Van Pham, T. H., Lu, P., Aagaard, P., Zhu, C. & Hellevang, H., (2011). On the potential of CO_2–water–rock interactions for CO_2 storage using a modified kinetic model. *International Journal of Greenhouse Gas Control*, *5*(4), 1002-1015. https://doi.org/https://doi.org/10.1016/j.ijggc.2010.12.002

White, A. F. & Brantley, S. L., (2003). The effect of time on the weathering of silicate minerals: why do weathering rates differ in the laboratory and field? *Chemical Geology*, *202*(3), 479-506. https://doi.org/https://doi.org/10.1016/j.chemgeo.2003.03.001

Wolery, T. J., Jové-Colón, C. F., Rard, J., Sutton, M., Helean, K., Finch, B. & Nowak, J., (2007). *Qualification of Thermodynamic Data for Geochemical Modeling of Mineral–Water Interactions in Dilute Systems*.

Xu, T., Apps, J. A. & Pruess, K., (2005). Mineral sequestration of carbon dioxide in a sandstone–shale system. *Chemical Geology*, *217*(3-4), 295-318. https://doi.org/https://doi.org/10.1016/j.chemgeo.2004.12.015

Xu, T., Sonnenthal, E., Spycher, N. & Zheng, L., (2014). *TOUGHREACT V3.0-OMP Reference Manual: A Parallel Simulation Program for Non-Isothermal Multiphase Geochemical Reactive Transport*.

Youngman, K. J., (1988). *Hydrothermal alteration and thermal evolution of the Wairakei-Tauhara geothermal area* [PhD, University of Auckland]. Auckland, New Zealand.